Journal of Membrane Science 578 (2019) 10–15

Contents lists available at ScienceDirect

Journal of Membrane Science

journal homepage: www.elsevier.com/locate/memsci

A membrane with ion fluxes responsive to temperature, pH and voltage

Quan Yang[a,b,*], William I. Whiting[a], Riccardo Dettori[a]

[a] Sandia National Laboratories, Livermore, CA, 94551-0969, United States
[b] Department of Chemical Engineering, Virginia Polytechnic Institute and State University, Blacksburg, 24061, United States

ARTICLE INFO

Keywords:
Membrane
Nanogate
Temperature-
pH- and voltage-responsive
Self-assembly

ABSTRACT

Cell membranes of biological cells embedded with nuclear pore complexes (NPCs) are capable of controlling the flow of ions, e.g. Na^+, K^+ and Ca^{2+} by responding to stimuli, e.g. pH and voltage. From the inspiration of NPCs, researchers have been endeavoring to develop nanogates to achieve the control of ion transport, but the developed nanogates only have a low selectivity, the factor of change (FC) in ion fluxes due to ON/OFF switching. To our knowledge, nanogates with high responsiveness to temperature changes have not been reported. As such membranes etched with nanopores having a high selectivity (FC) and the reversible gating of temperature, pH and voltage were to be developed in the work. The nanogates were modified with DNA strands, whose linkers, the six nucleobases at 3′ ends, are complementary. According to the experimental results, at mildly acidic pH values, e.g. pH 5.3, the prepared nanogate is in an open state, while at neutral pH values, e.g. pH 7.9, it is shut off. The change in ion fluxes is up to a factor of 90, which is remarkably high compared to other nanogates reported. It is observed experimentally that promoting the number of the complementary nucleobases at the 3′ ends of the strands would improve nanogate performance significantly, while varying the other nucleobases exerts little effects. Hence the formation of nucleobase pairs among the complementary nucleobases at the 3′ ends of the strands leads to the binding of various strands, self-assembly of a strand web and blockage of ion transport. When the temperature is increased, due to the promotion of the thermal motion of DNA strands, the nucleobase pairs and the strand web will not be generated and the nanogate will remain open even at pH 7.9. Hence the nanogate developed is capable of responding to temperature changes. Further experiments were performed to investigate the influence of the NaCl concentrations and small opening diameters exerted on nanogate performance.

1. Introduction

It is significant for all living creatures that flow of ions, e.g. Na^+, K^+ and Ca^{2+}, through nuclear membranes with nuclear pore complexes (NPCs) is in a controlled manner. Voltage-gated NPCs have strands consisting of amino acid residues at the inside walls of the nanopores [1]. Owing to the inspiration obtained from NPCs, researchers work diligently to develop nanoscale structures with selectivity for applications in small nanoscale devices such as nanofluidics, biosensors, etc. [2–13] though ion transport mechanism in NPCs has not been fully deciphered. Zhang et al. [14] and other researchers [15–18] built nanopores responsive to pH via attaching the wall of a nanopore with polymers that shrink or swell at various pH values. Some researchers [19–21] developed “smart” membranes, such as gel-blended membranes and polymer-grafted membranes. Tufania and Ozaydin [22] developed smart membranes that could only be used to modulate the flux of macromolecules, e.g. proteins, not ions. Wang et al. [23] and Liu et al. [24] reported smart membranes with nanogates modulating flux of water, not ions. Harrel et al. [25] developed a nanogate, with voltage gating, consisting of negatively charged DNA strands attached at the pore entrance. Xia et al. [26] constructed pH-responsive nanopores modified with DNA molecules. For nanogates or membranes developed for modulating ion flux in these researches, the change in ion flux caused by nanogate opening and closure is merely up to a factor of about 10. None were reported to be responsive to temperature changes. But nanogates that can achieve higher change in ion flux are urgently needed for applications such as drug release, where nanopores with diameters around 10 nm are employed [26–29]. Most of the polymers or DNA molecules applied to modify nanopore walls are limited to homo-sequences and the structures of the developed nanogates are simple, but advanced functions can only be fulfilled by delicate structures and building highly structured nanogates is essential for the obtainment of the full potential of smart nanopores [30]. In the research, we employed complicated DNA strands to modify the nanogate.

* Corresponding author. Sandia National Laboratories, Livermore, CA, 94551-0969, United States.
E-mail address: quanyangresearch@hotmail.com (Q. Yang).

https://doi.org/10.1016/j.memsci.2019.02.024
Received 23 July 2018; Received in revised form 10 February 2019; Accepted 11 February 2019
Available online 14 February 2019
0376-7388/ Published by Elsevier B.V.

Engineering delicate nanostructures is remarkably challenging because all nanoscale components should be placed at the right place in narrow nanopores [30]. The only solution is to let the polymers or DNA molecules self-assemble into delicate structures, as the protein components of NPCs do [31,32]. Nowadays, the self-assembly technique is widely employed to construct structures in nanoscale [33–41]. In the work, the self-assembly technique was adopted to assemble the strand web with DNA strands attached at nanopore walls.

In the research, membranes etched with nanopores having reversible gating of temperature, pH and voltage were developed successfully. The selectivity of the membranes is higher than other reported "smart" membranes. People use processes, e.g. self-assembly, chemical vapor deposition, etc. for scaled-up manufacturing of nanoscale devices to be applied for beyond a lab level, which is known as nanomanufacturing. Nanomanufacturing involves scaled-up, reliable, and cost-effective manufacturing of nanoscale materials, structures, devices, and systems. In the research, we used self-assembly process to build nanogates in membranes, so it is ready to be applied for scaled-up nanomanufacturing.

2. Experimental and computational methods

2.1. Fabrication of a membrane etched with nanopores

The nanopores in the shape of a cone were constructed in 12 μm polyethylene terephthalate (PET, Hostaphan RN12 Hoechst, 12 μm thick) foil using a track-etching technique [15,42,43]. During the etching process, the PET foil was fixed between two chambers similar to that in Fig. 1, which shows the experimental setup for ion flux-voltage curve measurements of ion flow through nanogates. Etchant on the left side of the foil was 7 M NaOH, while the chamber of the right side was filled with a solution of 1 M KCl and 1 M HCOOH. The etching process was controlled according to the magnitude of the ion current through the nanopores. The etched membranes were then put in Milli-Q water to remove residual salts. The diameters of the small openings of the prepared nanogates were determined with the method of firstly depositing gold within the nanopores prepared, then dissolving PET to free the deposited gold cone and finally imaging the gold cone with SEM.

Following the technique above, a membrane etched with 25 nanopores was prepared, as presented in Fig. 1(a). The average distance between neighbor nanopores is 7.5 μm.

2.2. Attachment of DNA strands

DNA strands were attached to the carboxyl groups of the nanopore inside walls via the amino group at the 5′ terminus of the strand using the process as follows.

Solution of DNA strands with a concentration of 1.5 mM was prepared by dissolving oligomer strands (New England Biolabs) in 100 mM MES buffer at pH 5.5. Certain amount of *N*-(3-Dimethylaminopropyl)-N′-ethylcarbodiimide (EDC) was added to the solution to achieve a concentration of 0.05 M. The small opening of the cone-shaped nanopore was in contact with the solution of DNA strands and EDC above while the large opening of the nanopore was in contact with a MES buffer solution. The attachment of DNA strands was hence carried out asymmetrically and the DNA strands were only attached to the region around the small opening of the nanopore [44].

2.3. Ion flux – voltage curve measurements

As presented in Fig. 1(b), the ion flux-voltage curve was obtained with a Keithley 6487 picoammeter (Keithley Instruments) to investigate the properties of the strand-modified nanogate. The averaged current I through one nanogate is calculated by dividing the total current read by the picoammeter by the number of the nanogates. Each test was redone

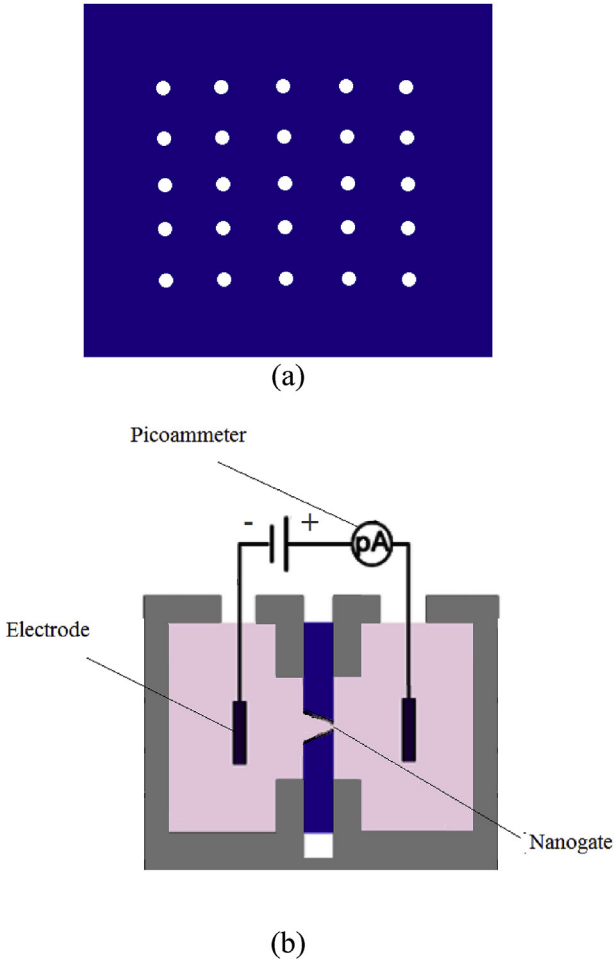

Fig. 1. (a) A PET membrane etched with 25 cone-shaped nanogates. (b) The experimental setup for the measurement of the ion flux-voltage curve of ion flow through nanogates.

five times to achieve the averaged values. With the averaged current I, $\frac{I}{e}$ and $\frac{I}{e \cdot N_A}$ give the number of ions transported through one nanogate per unit time and the ion flow rate, respectively. e and N_A are the absolute value of the charge of an electron, $1.602 \times 10^{-19} C$ and Avogadro constant, $6.022 \times 10^{23} mol^{-1}$, respectively. Then the ion flux can be evaluated with the following equation:

$$q = \frac{I}{e \cdot N_A \cdot A} \tag{1}$$

where A is the area of the small opening of the cone-shaped nanogate.

The selectivity of the membrane is estimated with the factor of change in ion flux due to ON/OFF switching of the nanogates according to Eq. (2):

$$S = \frac{q_{OPEN}}{q_{CLOSE}} \tag{2}$$

A *trans*-PET foil voltage was applied with Ag/AgCl electrodes. The electrode connected to the anode of the power supply faced the large openings of the nanopores, while that linked to the cathode faced the small ones. The nanogates were characterized by higher ion flux at the voltage applied with the electrodes, than at the voltage of the same value but in the reverse direction. Hence the voltage applied in Fig. 1 was exactly in the direction of the rectification of ion currents.

2.4. Contact angles (CA) measurements

CA measurements were done to characterize the membranes. At room temperature and saturated humidity we determined contact angles with an OCA 25 instrument (DataPhysics Instruments, Germany). The optical contact angle measuring and contour analysis systems of the OCA 25 are high precision optical measuring devices for the measurement of interfacial parameters and phenomena. We used MilliQ water as the source for the CA measurement. A 2-μL droplet of water was dispensed onto the substrates under investigation for each measurement.

2.5. Ion flux – voltage curve measurements

X-ray photoelectron spectroscopy (XPS) measurement was done to characterize chemical compositions of the membranes. XPS measurement was performed on the PHI 560 XPS Ultra High Vacuum (UHV) System (Physical Electronics Inc. (PHI), USA) using 200 W monochromated Al Kα radiation. For XPS analysis we used the 500 μm X-ray spot. In the analysis chamber the pressure was about 1×10^{-10} mbar. We employed the C1s binding energy at 285 eV for energy referencing. We used the peak of nitrogen (N1s) to reflect the DNA strands modification process.

3. Results and discussion

Fig. 2 shows the schematic plot of a slice of the nanogate we designed, viewed along the nanopore axis. The pore is in the shape of a cone as presented in Fig. 1(b), and the inside wall of the pore is attached with two types of DNA strands, i.e. (NH_2)-$(CH_2)_5$-(5′) -TGTTGG TTGGTG TGTGGG TGGTTG TATATA-(3′) and (NH_2)-$(CH_2)_5$-(5′)-TGTTGG TTGGTG TGTGGG TGGTTG ATATAT-(3′), where A, T, G and C represent nucleobases adenine, thymine, guanine and cytosine, respectively. The difference in the two types of DNA strands lies in the six nucleobases at the 3′ terminus, with one being TATATA-(3′) and the other being ATATAT-(3′), complementary to each other.

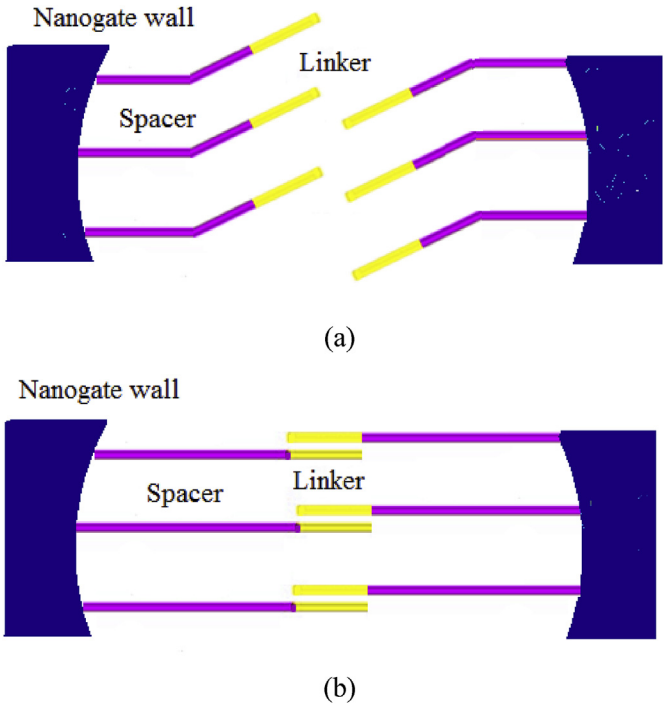

Fig. 2. The schematic plot of a slice of the nanogate. (a) At pH 5.3, no connections between linkers. (b) At pH 7.9, connections between linkers are established and a strand web is assembled, blocking ion transport. Linker: TATATA-(3′) or ATATAT-(3′), complementary to each other, with nearly the same amount, spacer: (NH_2)-$(CH_2)_5$-(5′)-TGTTGG TTGGTG TGTGGG TGGTTG.

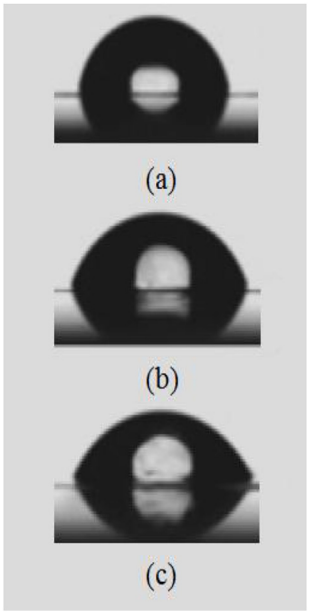

Fig. 3. The graphs of water droplet shape on (a) naked, (b) etched and (c) DNA strands-modified PET membranes. The contact angles of water droplet on naked, etched and DNA strands-modified PET membranes are 84.5°, 71.3°, 61.7° respectively.

The amino group at the 5′ terminus of the strand is to attach to the carboxyl group at the nanopore inside walls. Fig. 2 presents how DNA strands get linked with one another via linkers and spacers. The linker section of a strand is the six nucleobases at the 3′ terminus of the strand, i.e. TATATA-(3′) for one type and ATATAT-(3′) for the other type, with nearly the same amount, while the spacer section of the strand is the other part of the strand, i.e. (NH_2)-$(CH_2)_5$-(5′)-TGTTGG TTGGTG TGTGGG TGGTTG. At pH 5.3, linkers are designed not to bind with one another, while at pH 7.9, linkers will get interlinked to one another and a strand web is to be assembled, blocking ion transport.

The wall material is PET, a polyester, which is widely applied to generate a charged surface [45]. Etching of PET leads to the generation of carboxylate groups (COO^-) in the density of around one carboxylate group per unit nm^2 [46]. Diameters of the small opening (tip) of the created nanopores range from 6 nm to 17 nm. The technique employed for the attachment of the DNA strands to the inner wall of nanopores is presented in the section of experimental and computational methods.

Fig. 3 shows the graphs of water droplet shape on the PET membrane before and after modification with DNA strands. The contact angles of water droplet on naked, etched and DNA strands-modified PET membranes are 84.5°, 71.3°, 61.7° respectively. The changes in wettability of the PET membrane show the change in microstructures and chemical compositions of the membranes.

Fig. 4 shows the XPS spectra of the PET membrane after the modification with DNA strands and the inset presents the XPS spectra of the PET membrane before the modification. It is observed that there is a peak at the binding energy of 400 eV after the modification. It is a typical N1s XPS peak, demonstrating that DNA strands are attached on PET membrane.

The picoammeter in Fig. 1(b) gives currents corresponding to various voltages, from which the ion fluxes can be calculated with Eq. (1). The ion flux-voltage curves for the nanogate with a small opening of 10 nm are presented in Fig. 5. The voltage is the potential difference between the two openings of the nanopores and the flux is the ion flux through that. The results indicate that at pH 5.3, the ion flux increases nearly quadratically with the increase of the voltage and the gate is in

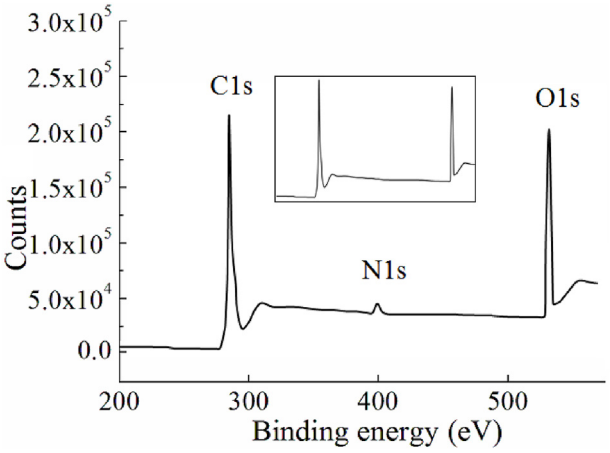

Fig. 4. The XPS spectra of the PET membrane after the modification with DNA strands. The inset shows the XPS spectra of the PET membrane before the modification with DNA strands.

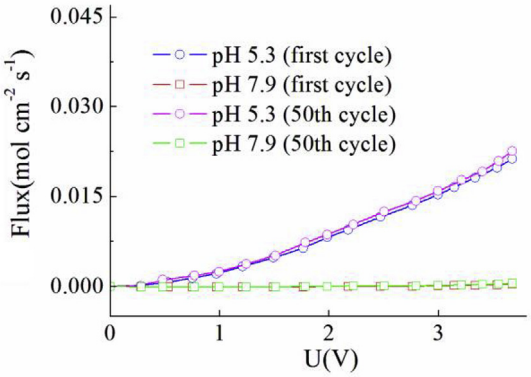

Fig. 5. The measured ion flux-voltage curve for the nanogate with a diameter of 10 nm (NaCl concentration: 125 mM) for the first cycle and the 50th cycle of experiments where the pH cycles between 5.3 and 7.9 and nanogates in the membrane are switched on and off repeatedly.

an open state, while at pH 7.9, the ion flux remains nearly zero for various voltages and the gate is shut off. The ion flux changes by a factor of around 90, remarkably high compared to other nanogates reported.[13−19] The nanogates were switched on and off repeatedly before the measurements of ion flux-voltage curves were redone. Fig. 5 also shows the measured ion flux-voltage curve for the 50th cycle of experiments. For the two cases, the difference in the ion fluxes corresponding to a voltage of 3 V at pH 5.3 is only 5%, so the reversibility of the membrane is robust.

The mechanism behind the gating is complicated. At pH 7.9, the DNA strands are negatively charged and repulsive interactions between strands would exert inclination for the 3′ ends of the strands to extend into the center phase of the nanogates, providing opportunity for the linkers of various strands to approach one another and subsequently get linked via hydrogen bonding interactions. DNA strand webs would therefore be constructed, leading to the blockage of ion transport and closure of the nanopores. On the contrary, at pH 5.3, the amount of negatively charged phosphate groups would decrease by a factor of around several tens. Additionally, no hydrogen bonds are formed and the 3′ ends of various strands are not get linked, causing no DNA strand webs assembled.

Then the influence of DNA nucleobase sequences on nanogate performance was researched and the results are presented in Fig. 6, which shows that of the three groups of DNA strands with various linkers:

(NH_2)-$(CH_2)_5$-(5′) -TGTTGG TTGGTG TGTGGG TGGTTG GGTATA-(3′) and (NH_2)-$(CH_2)_5$-(5′) -TGTTGG TTGGTG TGTGGG TGGTTG GGATAT-(3′)

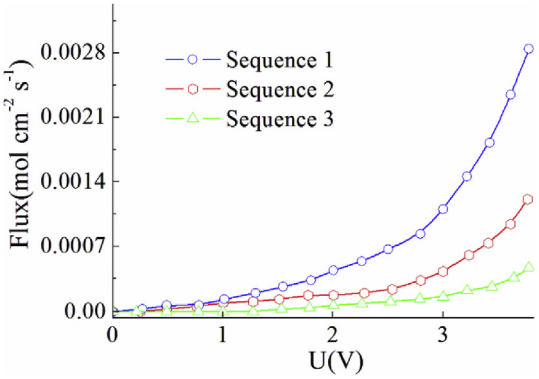

Fig. 6. Ion flux-voltage curve measurement results for nanogates with strands of three various DNA nucleobase sequences (pH: 7.9, NaCl concentration: 125 mM).

(NH_2)-$(CH_2)_5$-(5′) -TGTTGG TTGGTG TGTGGG TGGTTG GATATA-(3′) and $(NH_2$-$(CH_2)_5$-(5′) -TGTTGG TTGGTG TGTGGG TGGTTG GTATAT-(3′)

(NH_2)-$(CH_2)_5$-(5′) -TGTTGG TTGGTG TGTGGG TGGTTG TATATA-(3′) and (NH_2)-$(CH_2)_5$-(5′) -TGTTGG TTGGTG TGTGGG TGGTTG ATATAT-(3′)

The nanogates modified with the third groups of DNA strands perform best. Complementary nucleobases at the 3′ ends form hydrogen bonds and the longer the linkers are, the higher the number of formed hydrogen bonds would be. The third strand is capable of establishing the highest number of hydrogen bonds, so the strand web assembled is the strongest and the corresponding nanogates perform best.

The nanogates attached with these six groups of DNA strands with various spacers were prepared:

(NH_2))-$(CH_2)_5$-(5′) -TGTTGG TTGGTG TGTGGG TGGTTG TATATA-(3′) and (NH_2))-$(CH_2)_5$-(5′) -TGTTGG TTGGTG TGTGGG TGGTTG ATATAT-(3′)

(NH_2))-$(CH_2)_5$-(5′) -TTGGTG TGGGTG TGTGTG GGGGGG TATATA-(3′) and (NH_2))-$(CH_2)_5$-(5′) - TTGGTG TGGGTG TGTGTG GGGGGG ATATAT-(3′)

(NH_2))-$(CH_2)_5$-(5′) - TGTGTG GGGGGG TGTGGG TGGTGG TATATA-(3′) and (NH_2))-$(CH_2)_5$-(5′) - TGTGTG GGGGGG TGTGGG TGGTGG ATATAT-(3′)

(NH_2))-$(CH_2)_5$-(5′) - GGGGGG TGTGTG TTTTTT TGGTGG TATATA-(3′) and (NH_2))-$(CH_2)_5$-(5′) - GGGGGG TGTGTG TTTTTT TGGTGG ATATAT-(3′)

(NH_2)v(5′) - TTTGGG GGGTTT TTTGGG GGGTTT TATATA-(3′) and (NH_2))-$(CH_2)_5$-(5′) - TTTGGG GGGTTT TTTGGG GGGTTT ATATAT-(3′)

(NH_2))-$(CH_2)_5$-(5′) - TTTGTG GGGGGG TTTGGG TGGGGG TATATA-(3′) and (NH_2))-$(CH_2)_5$-(5′) - TTTGTG GGGGGG TTTGGG TGGGGG ATATAT-(3′)

The experimental results indicate that the nanogates with strands of these nucleobase sequences have nearly the same performance. So the spacers, the nucleobases besides the complementary nucleobases at the 3′ ends, do not contribute to gate closure as they do not form hydrogen bonds to assemble the strand web. Hence it is concluded that the complementary nucleobases at the 3′ ends, the linkers, matter most and determine the number of hydrogen bonds formed and the strongnessv of the assembled strand web.

The influence of the temperature was explored then. At pH 7.9, with the variation of the temperature from 25 °C to 50 °C, due to improved thermal motion of complex stands, the CC^+ nucleobase pairs and thereafter strand web would not be assembled and the nanogate would remain open, as presented in Fig. 7. To our knowledge, we are among the earliest to report nanogates with high responsiveness to temperature changes. Then at a temperature of 25 °C, the nanogate was closed

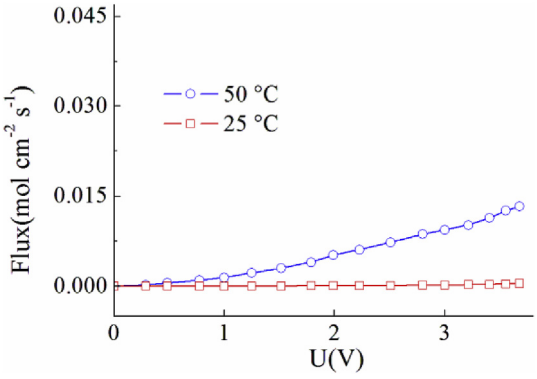

Fig. 7. Measured ion flux-voltage curves for the nanogate with a diameter of 10 nm at pH 7.9 at various temperature (NaCl conc)-$(CH_2)_5$-entration: 125 mM).

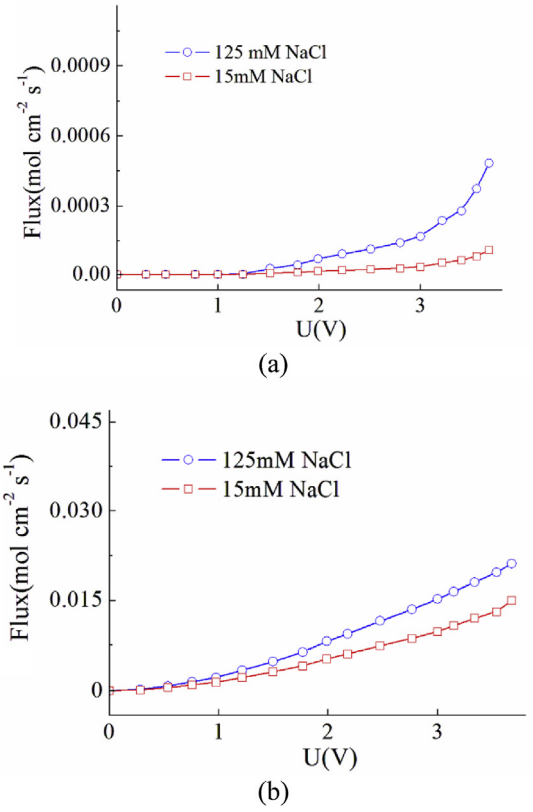

Fig. 8. Ion flux-voltage curves for the nanogate with a diameter of 10 nm in NaCl of various concentrations at (a) pH 7.9 and (b) pH 5.3, respectively.

and at 50 °C, the nanogate was switched on again, so the temperature-induced closure and opening of the nanogate is robust and reversible.

The research results for the influence of salt concentration are presented in Fig. 8. At pH of both 5.3 and 7.9, lowering salt concentration causes decreased ion transport flux, due to the interaction between strands becoming stronger and the formed strand web getting tight. Therefore the nanogate is characterized by improved responsiveness to voltage with the decrease of salt concentration.

Finally the performance of nanogates with various small opening sizes was studied and the results are presented in Fig. 9. The nanogates with small openings of 6 nm and 10 nm perform well. At pH 5.3, they are in the open state, while at pH 7.9, they are closed. But for the nanogate with a small opening of 17 nm, at pH 7.9, the ion flux is not low enough, being 3.1 times of that for the nanogate with an opening of 10 nm. The explanation is that the diameter of the small opening of the nanogate is so high that the strand web assembled is too loose to let the

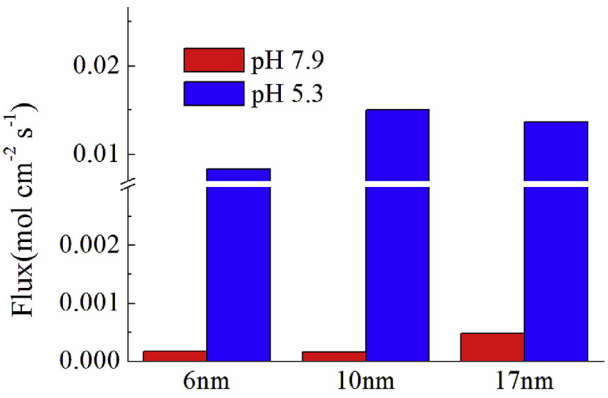

Fig. 9. Ion fluxes corresponding to a 3 V voltage between the two openings of nanogates with various small opening sizes. (NaCl concentration: 125 mM).

nanogate have the same performance as the nanogate with a 10 nm opening.

4. Conclusions

In biological cells, nuclear pore complexes (NPCs) are capable of controlling the flow of ions, e.g. Na^+, K^+ and Ca^{2+}. Though transport mechanism in NPCs has not been fully deciphered, researchers have been working to develop artificial nanogates to be applied in new devices such as biosensors and drug deliverers, but the selectivity, the factor of change in ion fluxes of the developed nanogates due to ON/OFF switching is low. The cone-shaped nanopores were constructed in 12 μm PET membranes using a track-etching technique. DNA strands were then attached to the carboxyl groups of the nanopore inside walls via the amino group at the 5′ terminus of the strands. According to the ion flux-voltage curves measured for the nanogate with a diameter of 10 nm, at pH 5.3, the nanogate is switched on, while at pH 7.9, the nanogate is shut off. The change in ion fluxes is up to factor of 90, which is remarkably high. In addition, the gating of the pH and voltage has reversibility. At pH 7.9, linkers form nucleobase pairs and DNA strands get linked, leading to the self-assembly of the strand web and blockage of ion transport. Then DNA nucleobase sequence influence on nanogate performance was researched. The results indicate that nanogates with strands of the longest linkers perform best and nucleobase sequences of the other section of a strand have no influence on gate performance. It is the length of the linkers that matter most and determine the number of hydrogen bonds formed and the strongness of the assembled strand web. At pH 7.9, when the temperature is increased, due to improved thermal motion of complex stands, the nucleobase pairs and thereafter strand web would not be generated and the nanogate would fail to be closed. To our knowledge, we are among the earliest to report nanogates with high responsiveness to temperature changes. Then the influence of salt concentration on nanogate performance was investigated. The nanogate responsiveness to voltage decreases with the increase of salt concentration. Finally the performance of nanogates with various diameters was studied. Nanogates with a small opening of 6 nm and 10 nm perform well, while for the nanogate with a small opening of 17 nm, at pH 7.9, the ion flux corresponding to a voltage of 3 V is 3.1 times of that for the 10 nm nanogate, because the diameter of the small opening of the nanogate is so high that the strand web assembled is loose.

In sum, in the research, membranes etched with nanopores having higher selectivity than other reported “smart” membranes were developed successfully. Those “smart” membranes are not as delicate as ours. For our membranes, the hydrogen bonding between DNA strands at mildly acidic pH values is strong enough to switch off the nanogates in membranes tightly, and the disappearance of the hydrogen bonding at neutral pH values ensures effective opening of the nanogates. So the

membranes developed have a high selectivity. Furthermore, as membranes modified with DNA strands are more delicate, they have more versatility to meet requirements of various applications than other “smart” membranes.

References

[1] B. Hille, Ionic Channels of Excitable Membranes, second ed., Sinauer Associates, Sunderland, Mass. USA, 1992.
[2] L.-J. Liang, Z.-S. Zhang, J.-W. Shen, X.-Y. Liu, Pressing carbon nanotubes triggers better ion selectivity, J. Phys. Chem. C 121 (2017) 19512–19518.
[3] C. Xu, C. Lei, L.-L. Huang, J. Zhang, H.-W. Zhang, H. Song, M.-H. Yu, Y.-D. Wu, C. Chen, C.Z. Yu, Glucose-responsive nanosystem mimicking the physiological insulin secretion via an enzyme–polymer layer-by-layer coating strategy, Chem. Mater. 29 (18) (2017) 7725–7732.
[4] A. de la Escosura-Muniz, A. Merkoci, Nanochannels Preparation and application in biosensing, ACS Nano 6 (2012) 7556–7583.
[5] C.R. Martin, Z.S. Siwy, Learning nature's way: biosensing with synthetic nanopores, Science 317 (2007) 331–332.
[6] J. Florek, R. Caillard, F. Kleitz, Evaluation of mesoporous silica nanoparticles for oral drug delivery - current status and perspective of MSNs drug carriers, Nanoscale 9 (2017) 15252–15277.
[7] L.T. Sexton, L.P. Horne, C.R. Martin, Developing synthetic conical nanopores for biosensing applications, Mol. Biosyst. 3 (2007) 667–685.
[8] I. Vlassiouk, T.R. Kozel, Z.S. Siwy, Biosensing with nanofluidic diodes, J. Am. Chem. Soc. 131 (2009) 8211–8220.
[9] A.B. Farimani, K. Min, N.R. Aluru, DNA base detection using a single-layer MoS_2, ACS Nano 8 (2014) 7914–7922.
[10] T. Jovanovic-Talisman, J. Tetenbaum-Novatt, A.S. McKenney, A. Zilman, R. Peters, M.P. Rout, B.T. Chait, Artificial nanopores that mimic the transport selectivity of the nuclear pore complex, Nature 457 (2009) 1023–1027.
[11] H. Daiguji, Ion transport in nanofluidic channels, Chem. Soc. Rev. 39 (2010) 901–911.
[12] A. Mourot, M.A. Kienzler, M.R. Banghart, T. Fehrentz, F.M.E. Huber, M. Stein, R.H. Kramer, D. Trauner, Tuning photochromic ion channel blockers, ACS Chem. Neurosci. 2 (9) (2011) 536–543.
[13] Y. Okamura, Y. Fujiwara, S. Sakata, Gating mechanisms of voltage-gated proton channels, Annu. Rev. Biochem. 84 (2015) 685–709.
[14] H. Zhang, X. Hou, L. Zeng, F. Yang, L. Li, D. Yan, Y. Tian, L. Jiang, Bioinspired artificial single ion pump, J. Am. Chem. Soc. 135 (2013) 16102–16110.
[15] S.P. Adiga, D.W. Brenner, Stimuli-responsive polymer brushes for flow control through nanopores, J. Funct. Biomater. 3 (2012) 239–256.
[16] B. Yameen, M. Ali, R. Neumann, W. Ensinger, W. Knoll, O. Azzaroni, Single conical nanopores displaying pH-tunable rectifying characteristics manipulating ionic transport with zwitter ionic polymer brushes, J. Am. Chem. Soc. 131 (2009) 2070–2071.
[17] G.H. de Groot, M.G. Santonicola, K. Sugihara, T. Zambelli, E. Reimhult, J. Vörös, G.J. Vancso, Switching transport through nanopores with pH-responsive polymer brushes for controlled ion permeability, ACS Appl. Mater. Interfaces 5 (2013) 1400–1407.
[18] X. Hou, F. Yang, L. Li, Y. Song, L. Jiang, D. Zhu, A biomimetic asymmetric responsive single nanochannel, J. Am. Chem. Soc. 132 (2010) 11736–11742.
[19] X.-B. Zhu, Y.-H. Zhou, J.R. Hao, B. Bao, X.-J. Bian, X.-Y. Jiang, J.-H. Pang, H.-B. Zhang, Z.-H. Jiang, L. Jiang, A charge-density-tunable three/two-dimensional polymer/graphene oxide heterogeneous nanoporous membrane for ion transport, ACS Nano 11 (2017) 10816–10824.
[20] C. Cheng, G. Jiang, C.J. Garvey, Y. Wang, G.P. Simon, J.Z. Liu, D. Li, Ion transport in complex layered graphene-based membranes with tuneable interlayer spacing, Sci. Adv. 2 (2016) e1501272.
[21] G. Jeon, S.Y. Yang, J.K. Kim, Functional nanoporous membranes for drug delivery, J. Mater. Chem. 22 (2012) 14814–14834.
[22] A. Tufania, G. Ozaydin, Protein gating by vapor deposited Janus membranes, J. Membr. Sci. 575 (2019) 126–134.
[23] Y. Wang, Z. Liu, F. Luo, H.-Y. Peng, S.-G. Zhang, R. Xie, X.-J. Ju, W. Wang, Y. Faraj, L.-Y. Chu, A novel smart membrane with ion-recognizable nanogels as gates on interconnected pores for simple and rapid detection of trace lead(II) ions in water, J. Membr. Sci. 575 (2019) 28–37.
[24] H.-W. Liu, J.-B. Liao, Y. Zhao, A. Sotto, J.-J. Zhu, B. van der Bruggen, C.-J. Gao, J.-N. Shen, Bioinspired dual stimuli-responsive membranes with enhanced gating ratios and reversible performances for water gating, J. Membr. Sci. 564 (2018) 53–61.
[25] C.C. Harrell, P. Kohli, Z. Siwy, C.R. Martin, DNA-nanotube artificial ion channels, J. Am. Chem. Soc. 126 (2004) 15646–15647.
[26] F. Xia, W. Guo, Y. Mao, X. Hou, J. Xue, H. Xia, L. Wang, Y. Song, H. Ji, Q. Ouyang, Y. Wang, L. Jiang, Gating of single synthetic nanopores by proton-driven DNA molecular motors, J. Am. Chem. Soc. 130 (2008) 8345–8350.
[27] S. Howorka, Z.S. Siwy, Nanopore analytics: sensing of single molecules, Chem. Soc. Rev. 38 (2009) 2360–2384.
[28] R. Duan, F. Xia, L. Jiang, Constructing tunable nanopores and their application in drug delivery, ACS Nano 7 (2013) 8344–8349.
[29] Q. Gao, Y. Xu, D. Wu, W. Shen, F. Deng, Synthesis characterization and in vitro pH-controllable drug release from mesoporous silica spheres with switchable gates, Langmuir 26 (2010) 17133–17138.
[30] K. Huang, I. Szleifer, Design of multifunctional nanogate in response to multiple external stimuli using amphiphilic diblock copolymer, J. Am. Chem. Soc. 139 (2017) 6422–6430.
[31] F. Alber, S. Dokudovskaya, L.M. Veenhoff, W.Z. Zhang, J. Kipper, D. Devos, A. Suprapto, O. Karni-Schmidt, R. Williams, B.T. Chait, M.P. Rout, A. Sali, Determining the architectures of macromolecular assemblies, Nature 450 (2007) 683–694.
[32] F. Alber, S. Dokudovskaya, L.M. Veenhoff, W. Zhang, J. Kipper, D. Devos, A. Suprapto, O. Karni-Schmidt, R. Williams, B.T. Chait, A. Sali, M.P. Rout, The Molecular architecture of the nuclear pore complex, Nature 450 (2007) 695–701.
[33] A.K. Thomas, R. Wieduwild, R. Zimmermann, W.-L. Lin, J. Friedrichs, M. Bickle, K. Fahmy, C. Werner, Y.-X. Zhang, Layer-by-layer assembly of heparin and peptide-polyethylene glycol conjugates to form hybrid nanothin films of biomatrices, ACS Appl. Mater. Interfaces 10 (2018) 14264–14270.
[34] S.-L. Xia, E. Metwalli, M. Opel, P.A. Staniec, E.M. Herzig, P. Müller-Buschbaum, Printed thin magnetic films based on diblock copolymer and magnetic nanoparticles, ACS Appl. Mater. Interfaces 10 (2018) 2982–2991.
[35] H.-C. Du, A. Cont, M. Steinacher, E. Amstad, Fabrication of hexagonal-prismatic granular hydrogel sheets, Langmuir 34 (2018) 3459–3466.
[36] H. Wang, E.D. Gomez, J. Kim, Z.-L. Guan, C. Jaye, D.A. Fischer, A. Kahn, Y.-L. Loo, Device characteristics of bulk-heterojunction polymer solar cells are independent of interfacial segregation of active layers, Chem. Mater. 23 (2011) 2020–2023.
[37] S.C. Larnaudie, J.C. Brendel, K.A. Jolliffe, S. Perrier, pH-Responsive, Amphiphilic core–shell supramolecular polymer brushes from cyclic peptide–polymer conjugates, ACS Macro Lett. 6 (2017) 1347–1351.
[38] W.-Y. Liu, M. Tagawa, H.L. Xin, T. Wang, H. Emamy, H.L. Li, K.G. Yager, F.W. Starr, A.V. Tkachenko, O. Gang, Diamond family of nanoparticle superlattices, Science 351 (2016) 582–586.
[39] I. Horin, T. Adiri, Y. Zafrani, Y. Cohen, Bis-resorcin[4]arene selectively forms hexameric capsules in apolar solvents: evidence from diffusion NMR, Org. Lett. 20 (13) (2018) 3958–3961.
[40] D.B. Lukatsky, B.M. Mulder, D. Frenke, Designing ordered DNA-linked nanoparticle assemblies, J. Phys. Condens. Matter 18 (2006) 567–571.
[41] A. Idili, A. Vallée-Bélisle, F. Ricci, Programmable pH-triggered DNA nanoswitches, J. Am. Chem. Soc. 136 (2014) 5836–5839.
[42] Y.A. Pavel, V.B. Irina, L.O. Oleg, R. Patricio, A.S. Bozena, Effect of nanopore geometry on ion current rectification, Nanotechnology 22 (2011) 175302.
[43] Z. Siwy, Y. Gu, H.A. Spohr, D. Baur, A. Wolf-Reber, R. Spohr, P. Apel, Y.E. Korchev, Rectification and voltage gating of ion currents in a nanofabricated pore, Europhys. Lett. 60 (2002) 349–355.
[44] H. Bayley, C.R. Martin, Resistive-pulse sensing-from microbes to molecules, Chem. Rev. 100 (2000) 2575–2594.
[45] C.A. Pasternak, C.L. Bashford, Y.E. Korchev, T.K. Rostovtseva, A.A. Lev, Modulation of surface flow by divalent cations and protons, Colloids Surf. A 77 (1993) 119–125.
[46] A. Wolf, N. Reber, P.Y. Apel, B.E. Fischer, R. Spohr, Nuclear instruments and methods in physics research, Nucl. Instrum. Methods B 105 (1995) 291–293.